Journal of Global Positioning Systems (*2021*)
Vol. 17, No. 2: 151-163
DOI: 10.5081/jgps.17.2.151

Multi-GNSS RTK positioning with integer ambiguity resolution: from double-differenced to single-differenced

Xiaolong Mi[1,2,3], Baocheng Zhang[2,4], Yunbin Yuan[2*]

1. School of Earth and Planetary Sciences, Curtin University, Perth, Australia
2. State Key Laboratory of Geodesy and Earth's Dynamics, Innovation Academy for Precision Measurement Science and Technology, Chinese Academy of Sciences, Wuhan, China
3. University of Chinese Academy of Sciences, Beijing, China
4. State Key Laboratory of Satellite Navigation System and Equipment Technology, the 54th Research Institute of China Electronics Technology Group Corporation, Shijiazhuang, China

* Corresponding author: Yunbin Yuan, yybgps@whigg.ac.cn

Abstract

The development of global navigation satellite systems (GNSS), especially BeiDou navigation satellite system with global coverage (BDS-3), has brought benefits for high-precision positioning. Real-time kinematic (RTK) positioning based on double-differenced (DD) observations has been widely used in high-precision positioning as common errors are eliminated. However, the biases at the receiver-end, which can be dynamically constrained, are also eliminated during the DD process. Therefore, it makes sense to turn RTK from DD to single-differenced (SD) as the advantages of dynamic constraints of the receiver biases can be exploited. In this contribution, we first present RTK models based on DD observations suitable for short, medium and long baselines. Then, based on SD observations, the full-rank RTK models are constructed with the *S*-system theory. Using observations from GPS, BDS-3 and Galileo, we first demonstrate the short-term stability of receiver-related biases. The SD RTK positioning performance with the stability of those receiver-related biases regarding integer ambiguity resolution success rate and positioning accuracy are analyzed. With those biases, RTK can achieve high performance, and this is more advantageous in multi-GNSS scenarios.

Keywords: Real-time kinematic (RTK), double-differenced (DD), single-differenced (SD), integer ambiguity resolution (IAR), BeiDou-3, global coverage, receiver biases

Introduction

Global and regional satellite navigation systems are developing rapidly, offering excellent opportunities for scientific and engineering applications [Li et al. 2019; Pignalberi et al. 2019; Ruhl et al. 2017]. Currently, GPS, GLONASS and Galileo are undergoing modernization while BeiDou navigation satellite system (BDS-3) completed its global deployment in July 2020 [Karutin 2020; Liu et al. 2021; Yalvac and Berber 2018; Yang et al. 2021; Yuan et al. 2020]. The advent of regional navigation satellite systems (RNSS) such as quasi-zenith satellite system (QZSS) and Navigation Indian Constellation (NavIC) has also increased the number of satellites in orbit [Santra et al. 2019; Zaminpardaz et al. 2018]. More satellites and frequencies are becoming available in this situation that benefits

Editor in charge: Dr. Zhizhao Liu

positioning, navigation, and timing (PNT) applications.

Precise point positioning (PPP) and real-time kinematic (RTK) positioning are two representative techniques [Paziewski et al. 2018; Shi et al. 2020]. Based on precise orbit and clock products, PPP can provide centimeter-level positioning services [Bahadur and Nohutcu 2019]. However, traditional PPP solutions typically require a 5-30 min convergence period and do not consider integer ambiguity resolution, which is defective in real-time and high-precision applications [Xiao et al. 2019]. Some commercial high-precision services have reduced PPP convergence time to a few minutes, but this requires additional precise corrections [Atiz et al. 2021]. With the help of a reference network, RTK can achieve fast integer ambiguity resolution and thus provide millimeter-level positioning services. Although integer ambiguity resolution enabled PPP (PPP-RTK) as a new representative technology is attracting widespread attention [Khodabandeh and Teunissen 2016], RTK is still the technology which real-time high-precision GNSS services depend on.

The classical RTK is usually based on double-differenced (DD) observations, which can benefit from serval advantages. First, DD RTK eliminates common errors from both the receiver-end and satellite-end; thus, the full-rank model can be obtained directly. Second, errors in propagation such as ionospheric and tropospheric delays are greatly reduced during the DD process. However, the DD observations amplify the effect of observation noise and multipath effect. In addition, the DD model eliminates the biases at the receiver-end, thus losing the opportunity to impose dynamic constraints to enhance the model strength [Odolinski et al. 2015b]. There is a mathematical correlation between the DD observations, which is not conducive to quality control and judging the source of gross error [Zhang et al. 2019].

The advantages of a SD model compared with a DD one have already been recognized for a long time in the case of RTK positioning [Liu et al. 2003; Mi et al. 2019a; Odijk and Teunissen 2008; Odolinski et al. 2015a]. With an SD formulation, one has the advantage of using a more straightforward observational variance matrix than the one used in a DD formulation. Receiver-end biases that are not considered of interest in positioning are eliminated in a DD model while retained in an SD one, which a dynamic model can constrain to improve model strength [Mi et al. 2020]. Those receiver-related biases include differential code bias (DCB), differential phase bias (DPB) and inter-system bias (ISB). DCBs and DPBs are stable that can be pre-corrected or estimated as time-invariants, both of which can enhance the model strength. ISBs can promote the signal integration of multi-frequency and multi-constellation, which is beneficial to PNT in terms of accuracy, integrity, and availability [Odijk et al. 2017; Tian et al. 2019].

With the SD observations, rank deficiencies have to be solved as not all unknowns can be estimated without biases [Odolinski et al. 2020]. Fortunately, the *S*-system theory can be used to identify the source of rank defects, select appropriate *S*-basis and construct a full-rank model, which was developed for terrestrial geodetic networks at first [Odolinski and Teunissen 2017a]. It should be noted that the choice of *S*-basis is not unique, which dictates the estimability and the interpretation of parameters.

In this contribution, we first review the ionosphere-float, -weighted and -fixed DD RTK models considering different ionospheric constraints, suitable for long, medium and short baselines. Then, based on the SD observations, we propose the ionosphere-float, -weighted and -fixed SD RTK models. As for the rank deficiencies in the SD models, the *S*-system theory is used to construct the full-rank model.

The remainder of this paper proceeds as follows. Section 2 first reviews the DD RTK model and then develops the RTK model based on SD observations. Section 3 presents the experimental setup and RTK positioning results for GPS, BDS-3 and Galileo. Finally, we summarize our findings and conclusions in Section 4.

Methodology

This section first gives the DD RTK models suitable for short to long baselines, namely ionosphere-float, -weighted and -fixed model. Then, the SD RTK models of ionosphere-float, -weighted and -fixed are constructed.

GNSS observation equations

The starting point of developing RTK models is the equations for GNSS code and phase observables [Leick et al. 2015], which read, respectively

$$\begin{aligned} p_{r,j}^{s} &= \rho_r^s + \tau_r^s + dt_r - dt^s + \mu_j I_r^s + d_{r,j} - d_{,j}^s + \varepsilon_{p,r,j}^s \\ \phi_{r,j}^{s} &= \rho_r^s + \tau_r^s + dt_r - dt^s - \mu_j I_r^s + \lambda_j N_{r,j}^s + \delta_{r,j} - \delta_{,j}^s + \varepsilon_{\phi,r,j}^s \end{aligned} \quad (1)$$

with r , s and j the receiver, satellite and frequency. $p_{r,j}^{s}$ and $\phi_{r,j}^{s}$ are the code and phase observations measured by receiver r from satellite s on frequency j. ρ_r^s is the satellite-receiver range, τ_r^s is the tropospheric delay, dt_r is the receiver clock and $d_{r,j}$ ($\delta_{r,j}$) is the receiver code (phase) bias. I_r^s is the ionospheric delay and $\mu_j = \lambda_j^2 / \lambda_1^2$ is its coefficient with λ_j the wavelength, $N_{r,j}^s$ is the integer phase ambiguity. dt^s is the satellite clock and $d_{,j}^s$ ($\delta_{,j}^s$) is the satellite code (phase) bias. $\varepsilon_{p,r,j}^s$ and $\varepsilon_{\phi,r,j}^s$ are the code and phase observation noise and miss-modeled random effects.

DD RTK model

The common errors at the satellite-end and the receiver-end are eliminated in DD RTK without rank deficiency. Therefore, DD RTK can be directed used for precise positioning. Considering that different ionospheric delay processing strategies, three variants are given.

DD ionosphere-float variant

During the DD process, one receiver and one satellite have to be selected as pivot receiver and satellite (represented by 1). Then, the DD code and phase observations can be given as follows,

$$\begin{aligned} p_{1r,j}^{1s} &= \rho_{1r}^{1s} + \tau_{1r}^{1s} + \mu_j I_{1r}^{1s} + \varepsilon_{p,1r,j}^{1s} \\ \phi_{1r,j}^{1s} &= \rho_{1r}^{1s} + \tau_{1r}^{1s} - \mu_j I_{1r}^{1s} + \lambda_j N_{1r,j}^{1s} + \varepsilon_{\phi,1r,j}^{1s} \end{aligned} \quad (2)$$

where $p_{1r,j}^{1s}$ and $\phi_{1r,j}^{1s}$ are the DD code and phase observations, respectively. τ_{1r}^{1s} and I_{1r}^{1s} are the DD tropospheric and ionospheric delays. $N_{1r,j}^{1s}$ is the DD phase ambiguity. For long baselines, the DD tropospheric and ionospheric delays cannot be neglected. For tropospheric delay, it is common practice to divide it into two parts, dry and wet delays where $\tau_r^s = (\tau_d)_r^s + m_r^s \tau_r$. The dry part $(\tau_d)_r^s$ is directly corrected in the code and phase observations using an a-priori troposphere model [Leandro et al. 2008]. The wet part τ_r zenith troposphere delay (ZTD) is estimated as unknown with m_r^s an elevation-dependent mapping function [Hadas et al. 2020; Tuka and El-Mowafy 2013]. For the DD ionospheric delays, they are estimated as unknown parameters together with the other parameters in long baselines. Therefore, the DD ionosphere-float model can be given as

$$\begin{aligned} \tilde{p}_{1r,j}^{1s} &= \rho_{1r}^{1s} + m_r^{1s}\tau_{1r} + \mu_j I_{1r}^{1s} + \varepsilon_{p,1r,j}^{1s} \\ \tilde{\phi}_{1r,j}^{1s} &= \rho_{1r}^{1s} + m_r^{1s}\tau_{1r} - \mu_j I_{1r}^{1s} + \lambda_j N_{1r,j}^{1s} + \varepsilon_{\phi,1r,j}^{1s} \end{aligned} \quad (3)$$

with $\tilde{p}_{1r,j}^{1s} = p_{1r,j}^{1s} - (\tau_d)_{1r}^{1s}$ and $\tilde{\phi}_{1r,j}^{1s} = \phi_{1r,j}^{1s} - (\tau_d)_{1r}^{1s}$.

DD ionosphere-weighted variant

It is acceptable to use Eq. (3) for RTK positioning of medium baselines with no more than 100 kilometers. However, the ionospheric delays from the same satellite are approximately equal for the different receivers at this distance [Teunissen 1998]. Therefore,

it is wise to include the ionospheric delay in the model of Eq. (3) as an additional observable [Zha et al. 2021]. The DD ionosphere-weighted model can be given as follows,

$$\begin{aligned}\tilde{p}_{1r,j}^{1s} &= \rho_{1r}^{1s} + m_r^{1s}\tau_{1r} + \mu_j I_{1r}^{1s} + \varepsilon_{p,1r,j}^{1s} \\ \tilde{\phi}_{1r,j}^{1s} &= \rho_{1r}^{1s} + m_r^{1s}\tau_{1r} - \mu_j I_{1r}^{1s} + \lambda_j N_{1r,j}^{1s} + \varepsilon_{\phi,1r,j}^{1s} \\ \overline{I}_{1r}^{1s} &= I_{1r}^{1s} + \varepsilon_{I,1r,j}^{1s}\end{aligned} \quad (4)$$

where $\overline{I}_{1r}^{1s}$ is the DD ionospheric pseudo-observables, and can be interpolated by reference network or assumed as zero for medium baselines. The reasonable stochastic model of those observables is necessary, which is usually determined by both baseline length and satellite elevation angle. It is worth noting that the stochastic model is limited by the region and time, so it is necessary to model the stochastic model for the operating area in advance [Mi et al. 2019b].

DD ionosphere-fixed variant

For baselines within a few tens of kilometers, it is safe to assume the DD ionospheric and tropospheric delays are zero. Therefore, the DD ionosphere-fixed model can be written as,

$$\begin{aligned}\tilde{p}_{1r,j}^{1s} &= \rho_{1r}^{1s} + \varepsilon_{p,1r,j}^{1s} \\ \tilde{\phi}_{1r,j}^{1s} &= \rho_{1r}^{1s} + \lambda_j N_{1r,j}^{1s} + \varepsilon_{\phi,1r,j}^{1s}\end{aligned} \quad (5)$$

The unknown parameters to be estimated are position and phase ambiguity, and the strength of the model is improved.

SD RTK model

Unlike the DD RTK model, the SD model needs to be solved uniquely, as it is a rank-deficient system. This means that not all the unknowns in the SD model can be estimated separately, but only their combinations. Therefore, to construct the full-rank SD model, the *S*-system theory is used. The details of *S*-system theory can be referred to Odijk et al. [2016], which will not be repeated here. Similar to the DD model, ionosphere-float, -weighted and -fixed variants are constructed, respectively.

SD ionosphere-float variant

As a starting point of developing the SD algorithm, we first give the SD code and phase observations which reads,

$$\begin{aligned}p_{1r,j}^{s} &= \rho_{1r}^{s} + \tau_{1r}^{s} + dt_{1r} + \mu_j I_{1r}^{s} + d_{1r,j} + \varepsilon_{p,1r,j}^{s} \\ \phi_{1r,j}^{s} &= \rho_{1r}^{s} + \tau_{1r}^{s} + dt_{1r} - \mu_j I_{1r}^{s} + \lambda_j N_{1r,j}^{s} + \delta_{1r,j} + \varepsilon_{\phi,1r,j}^{s}\end{aligned} \quad (6)$$

where $p_{1r,j}^{s}$ and $\phi_{1r,j}^{s}$ are the SD code and phase observations. ρ_{1r}^{s} is the SD satellite-receiver range, τ_{1r}^{s} and I_{1r}^{s} are the SD tropospheric and ionospheric delays. dt_{1r} is the SD receiver clock, $d_{1r,j}$ and $\delta_{1r,j}$ are the SD receiver code and phase biases. $N_{1r,j}^{s}$ is the SD phase ambiguity.

Although the satellite clock, code and phase biases are eliminated during this process, Eq. (5) can still not be used for RTK positioning, as it is rank-deficient. The rank-deficient occurs in three ways [Mi et al. 2021; Odolinski and Teunissen 2016; Odolinski and Teunissen 2017b]. First, the linear dependency between the columns of the receiver clock and the receiver code/phase biases. Second, the column dependency between the receiver clock, the code/phase biases and the ionosphere delay. Third, the columns of the design matrix between the receiver phase bias and phase ambiguity are linear dependent. As we mentioned earlier, those rank deficiencies can be eliminated by the *S*-system theory. The first two rank deficiencies can be eliminated by fixing the SD receiver code biases on $j = 1$ ($d_{1r,1}$)and on $j = 2$ ($d_{1r,2}$), respectively. As for the third one, one satellite has to be selected as pivot satellite to overcome this rank deficiency.

Once the rank deficiencies have been solved, the full-rank SD ionosphere-float RTK model can be

given as,

$$\begin{aligned}\tilde{p}^s_{1r,j} &= \rho^s_{1r} + m^s_r\tau_{1r} + d\tilde{t}_{1r} + \mu_j\tilde{I}^s_{1r} + \tilde{d}_{1r,j} + \varepsilon^s_{p,1r,j}\\ \tilde{\phi}^s_{1r,j} &= \rho^s_{1r} + m^s_r\tau_{1r} + d\tilde{t}_{1r} - \mu_j\tilde{I}^s_{1r} + \lambda_j N^{1s}_{1r,j} + \tilde{\delta}_{1r,1} + \tilde{\delta}_{1r,j} + \varepsilon^s_{\phi,1r,j}\end{aligned} \tag{7}$$

where $\tilde{p}^s_{1r,j} = p^s_{1r,j} - (\tau_d)^s_{1r}$ and $\tilde{\phi}^{1s}_{1r,j} = \phi^s_{1r,j} - (\tau_d)^s_{1r}$, the dry tropospheric delay is directly corrected in the observations. The reparametrized estimable unknowns in Eq. (7) are given in Table 1.

Table 1 The reparametrized estimable unknowns and their interpretation for SD ionosphere-float model, where $d_{1r,GF} = \frac{1}{\mu_2-\mu_1}(d_{1r,2} - d_{1r,1})$ and $d_{1r,IF} = \frac{\mu_2}{\mu_2-\mu_1}d_{1r,1} - \frac{\mu_1}{\mu_2-\mu_1}d_{1r,2}$

Notation and interpretation	Estimable parameter	Conditions
$d\tilde{t}_{1r} = dt_{1r} + d_{1r,IF}$	Between-receiver clock	
$\tilde{d}_{1r,i} = d_{1r,i} - d_{1r,IF} - \mu_i d_{1r,GF}$	Between-receiver DCB	$j \geq 3$
$\tilde{\delta}_{1r,1} = \delta_{1r,1} - d_{1r,IF} + \mu_j d_{1r,GF} + \lambda_j N^1_{1r,1}$	Between-receiver DPB of the first frequency	
$\tilde{\delta}_{1r,i} = \delta_{1r,i} - \delta_{1r,1} + \lambda_i N^1_{1r,i} - \lambda_i N^1_{1r,1}$	Between-receiver DPB	$j \geq 2$
$\tilde{I}^s_{1r} = I^s_{1r} + d_{1r,GF}$	Between-receiver iono delays biased by receiver code bias	

SD ionosphere-weighted variant

With the ionosphere pseudo-observables available, the second rank deficiency gets eliminated, which increases the redundancy and thus strengthens the model. After the first and third rank deficiencies have been solved, the full-rank SD ionosphere-weighted RTK read,

$$\begin{aligned}\tilde{p}^s_{1r,j} &= \rho^s_{1r} + m^s_r\tau_{1r} + d\tilde{\tilde{t}}_{1r} + \mu_j I^s_{1r} + \tilde{\tilde{d}}_{1r,j} + \varepsilon^s_{p,1r,j}\\ \tilde{\phi}^s_{1r,j} &= \rho^s_{1r} + m^s_r\tau_{1r} + d\tilde{\tilde{t}}_{1r} - \mu_j I^s_{1r} + \lambda_j N^{1s}_{1r,j} + \tilde{\tilde{\delta}}_{1r,1} + \tilde{\tilde{\delta}}_{1r,j} + \varepsilon^s_{\phi,1r,j}\\ \overline{I}^s_{1r} &= I^s_{1r} + \varepsilon^s_{I,1r,j}\end{aligned} \tag{8}$$

where $\overline{I}^s_{1r}$ is the SD ionospheric pseudo-observables. The reparametrized estimable unknowns and their interpretation are different from the SD ionosphere-float model, which is presented in Table 2.

Table 2 Reparametrized estimable unknowns and their interpretation for the SD ionosphere-weighted and -fixed model

Notation and interpretation	Estimable parameter	Conditions
$d\tilde{\tilde{t}}_{1r} = dt_{1r} + d_{1r,1}$	Between-receiver clock	
$\tilde{\tilde{d}}_{1r,j} = d_{1r,j} - d_{1r,1}$	Between-receiver DCB	$j \geq 2$
$\tilde{\tilde{\delta}}_{1r,1} = \delta_{1r,1} - d_{1r,1} + \lambda_j N^1_{1r,1}$	Between-receiver DPB of the first frequency	
$\tilde{\tilde{\delta}}_{1r,j} = \delta_{1r,j} - \delta_{1r,1} + \lambda_j N^1_{1r,j} - \lambda_j N^1_{1r,1}$	Between-receiver DPB	$j \geq 2$

SD ionosphere-fixed variant

For short baselines, the SD ionospheric and tropospheric delays can be assumed as zero to strengthen the model. Similar to the SD ionosphere-weighted model, the SD ionosphere-fixed also needs to solve the first and third rank deficiencies. Thus, the *S*-basis choices are also the same as in the ionosphere-weighted model. The full-rank SD ionosphere-fixed model follows as,

$$\begin{aligned}\tilde{p}^{s}_{1r,j} &= \rho^{s}_{1r} + d\tilde{\tilde{t}}_{1r} + \tilde{\tilde{d}}_{1r,j} + \varepsilon^{s}_{p,1r,j} \\ \tilde{\phi}^{s}_{1r,j} &= \rho^{s}_{1r} + d\tilde{\tilde{t}}_{1r} + \lambda_j N^{1s}_{1r,j} + \tilde{\tilde{\delta}}_{1r,1} + \tilde{\tilde{\delta}}_{1r,j} + \varepsilon^{s}_{\phi,1r,j}\end{aligned} \tag{9}$$

where the estimable unknowns and their interpretation are also the same as in the Eq. (8) in Table 2.

Experimental Analysis

This section starts with an outline of the experimental setup, including the relevant characteristics of the experimental datasets considered for this study and our data processing strategies. Then, the characterization of the receiver-end biases, including DCB and DPB. Following that is an evaluation of the SD RTK positioning performance in terms of integer ambiguity resolution success rate and positioning accuracy.

Experimental setup

We collected multi-GNSS data from three receivers in Wuhan, China, including one Septentrio POLARx5 (APM3), one Septentrio POLARx5TR (APM7) at the campus of the Innovation Academy of Precision Measurement Science and Technology, Chinese Academy of Sciences and one JAVAD TRE_3 (WHU2) at the campus of Wuhan University. We connected the receivers (APM3 and APM7) to a single antenna that is 1.7 km away from WHU2. Those data were collected for GPS, BDS-3 and Galileo on June 9-10, 2021, with a sampling interval of 30 s. The detailed characteristics of the experimental data used in our study are summarized in Table 3.

Table 3 An overview of GNSS data considered in our study

Station ID	Receiver type	Antenna type	Constellation
APM3	Septentrio POLARx5	TRM159800.00 NONE	GPS L1, L2
APM7	Septentrio POLARx5TR		BDS-3 BIC, B2a
WUH2	JAVAD TRE_3	JAVRINGANT_G5T NONE	Galileo E1 E5a

The cut-off elevation was set to 15° to reduce the impact of the multipath effect, and the elevation-dependent weighting function was used [Shen et al. 2009]. GPS, Galileo, and BDS-3 are assumed to be equal-weighted, where the undifferenced zenith-referenced a priori code and phase standard deviations are 0.3 m and 0.003 m, respectively. The LAMBDA and the ratio test were used for integer ambiguity resolution and the validation of the correctness of the resolved ambiguities [Teunissen and Verhagen 2009; Teunissen et al. 1997]. In addition, the effect of the outliers was detected and eliminated through the Detection, Identification and Adaptation (DIA) procedure [Teunissen 2018].

Characterization of receiver-related biases

As we can see from those SD models, three receiver-related biases are included, including DCB, DPB of the first frequency and DPB. See the interpretation of the DPB of first frequency ($\tilde{\delta}_{1r,1} = \delta_{1r,1} + d_{1r,IF} - \mu_j d_{1r,GF} + \lambda_j N^1_{1r,1}$ in ionosphere- float model and $\tilde{\delta}_{1r,1} = \delta_{1r,1} + d_{1r,1} + \lambda_j N^1_{1r,1}$ in ionosphere-weighted

and fixed models), which contains a combination of code and phase biases. Thus, the DPB of the first frequency is influenced by code observations while the DPB, which is only related to phase observation, is not.

As a typical example, we show in Figs. 1-3 those three receiver-related biases for GPS, BDS-3 and Galileo with the zero baseline APM3-APM7 on June 9, 2021. The purpose of this is to characterize these biases to determine whether they can be pre-corrected or estimated as time invariants in RTK positioning. See Fig. 1 first, showing the DCB for GPS, BDS-3 and Galileo. Focusing on each panel, we can see that the DCB of all three systems is significant, which can not be ignored in RTK positioning. These DCB estimates fluctuate randomly around their mean values with no apparent trend over time. The standard deviations of DCB estimates for GPS, BDS-3 and Galileo are 0.029 m, 0.014 m and 0.019 m, exhibiting noise much smaller than the code observations with decimeter level. That is to say, DCB is stable enough over short-time, so it can be pre-corrected or used as time-invariant parameter estimation in RTK positioning.

Then turn attention to Fig.2, depicting the DPB of the first frequency. As the DPB of the first frequency is the difference between code and phase biases, its estimate has a similar noise level to DCB as expected. The standard deviations of DPB of the first frequency estimates for GPS, BDS-3 and Galileo are 0.025 m, 0.012 m and 0.015 m, slightly smaller than that of DCB. This is because DCB is the difference of the code bias between the second frequency and the first frequency, while DPB is the difference between the code bias and the phase bias of the first frequency, and the noise of the phase bias is less than the code one.

We confirm and extend our findings from Fig.3, showing the DPB estimates for GPS, BDS-3 and Galileo. First, those DPB estimates fluctuate randomly around their mean values, just like DCB and DPB of the first frequency, but with more negligible noise. The standard deviations of DPB of the first frequency estimates for GPS, BDS-3 and Galileo are below 1 mm, showing minimal noise. This is because that DPB is only related to phase observations with slight noise. However, DPB is more difficult to pre-correct due to the introduction of the ambiguity with two frequencies. Thus, the usual practice is to treat DPB as a time-invariant parameter in RTK positioning.

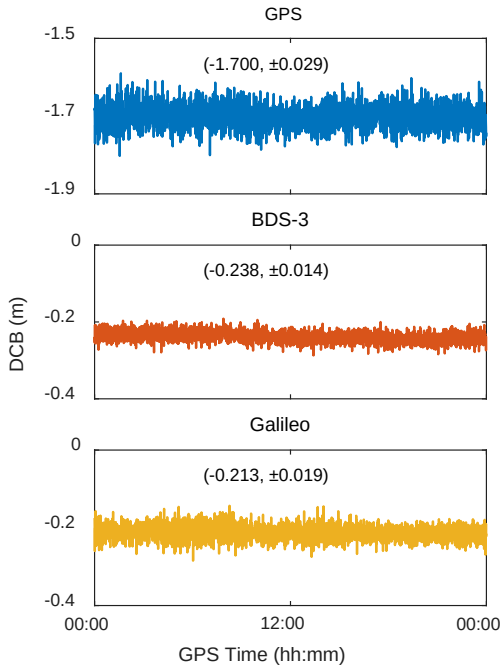

Fig. 1 Time series of DCB for APM3-APM7 with GPS, BDS-3 and Galileo on DOY 159 of 2021

SD RTK positioning performance

As we have shown above, receiver-related DCB, DPB of the first frequency and DPB have good short-term stability, thus can be estimated as time-invariants. Thus, for multi-frequency multi-GNSS RTK positioning, the SD method can achieve better performance than the DD method [Liu et al. 2004]. To test the performance of SD RTK, we select GNSS data from two baselines, a zero one (APM3-APM7) and a short one (APM7-WUH2) with 1.7 km, on June 10, 2021. In our analysis, receiver-related biases are estimated as time-invariants for each constellation, and the integer ambiguity resolution success rate and positioning accuracy are assessed.

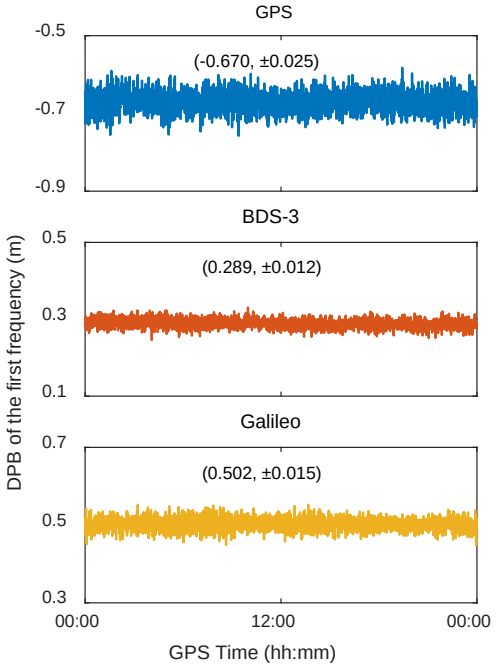

Fig. 2 Time series of DPB of the first frequency for APM3-APM7 with GPS, BDS-3 and Galileo on DOY 159 of 2021

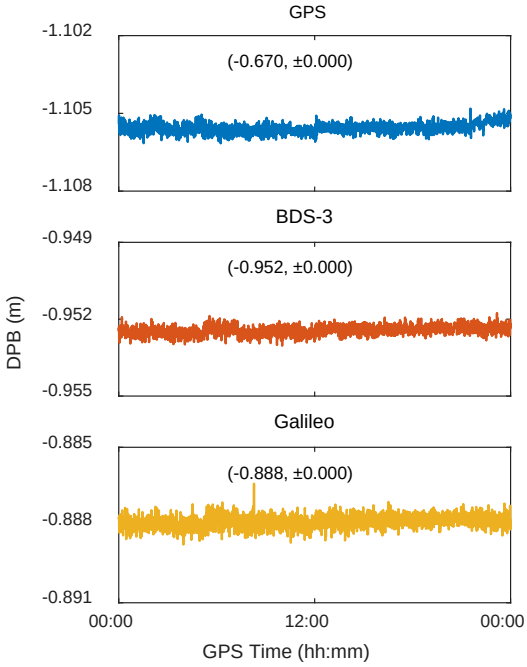

Fig. 3 Time series of DPB for APM3-APM7 with GPS, BDS-3 and Galileo on DOY 159 of 2021

Table 4 presents the integer ambiguity resolution success rate results with GPS, BDS-3, Galileo and their combination for APM3-APM7 and APM7-WUH2 on June10, 2021. Our analysis defines the success rate as the epochs with ambiguity corrected resolved divided by the total epochs. For zero baseline APM3-APM7, as the atmospheric delays are fully eliminated, the integer ambiguity resolution success rate for GPS-only, BDS-3-only, Galileo-only and their combination are all 100%. The short baseline APM7-WUH2, limited by atmospheric delays and multipath effect, does not achieve the same performance as the zero baseline APM3-APM7. The success rate for GPS-only, BDS-3-only, Galileo-only and GPS+BDS-3+Galileo is 96.7%, 97.1%, 95.2% and 99.7%. For a single constellation, the success rate of BDS-3 is higher than that of GPS and Galileo, which is owing to the more visible satellites of BDS-3 in China. With the combination of those three constellations, the success rate reaches 99.7%, demonstrating the advantages of multi-GNSS.

Fig. 4 shows the positioning results of the zero baseline APM3-APM7 with GPS, BDS-3, Galileo and GPS+BDS-3+Galileo on June 10, 2021. As we can see that BDS-3 achieves the highest positioning accuracy (1.6 mm, 1.9 mm and 4.1 mm for E, N, U) among three single constellations. This may be due to BDS-3 has more satellites observable in China than GPS and Galileo. For GPS+BDS-3+Galileo, the root-mean-square (RMS) of the positioning errors in the North/East/Up is 1.3 mm, 1.2 mm and 3.5 mm, better than the other three single constellations.

Fig. 5 depicts the positioning performance of the short baseline APM7-WUH2. The impact of residual atmospheric errors and multipath effects is shown in the positioning results, reflected in the RMS of positioning errors. For three single constellations, BDS-3 performs the best, followed by GPS and Galileo. The advantages of combining the three systems are also demonstrated, where the RMS of the positioning errors in the North/East/Up is 1.0.6 cm, 0.6 cm and 1.3 cm, respectively.

Conclusions

Real-time kinematic (RTK) positioning based on double-differenced (DD) observations has been wildly used. Although the DD RTK eliminates the

common parameters, it loses the opportunity to constrain some parameters dynamically. In this contribution, we focused on single differenced (SD) observations with receiver-end parameters. However, the RTK model based on SD observations is rank-deficient, so the *S*-system theory was used to construct the full-rank model. Considering different ionospheric constraints, we derived three SD models: ionosphere-float, -weighted and -fixed.

Table 4 Integer ambiguity resolution success rate for the zero baseline APM3-APM7 and the short baseline APM7-WUH2 with GPS, BDS-3 and Galileo on June 10, 2021

Constellation	APM3-APM7	APM7-WUH2
GPS	2880/2880=100%	2786/2880=96.7%
BDS-3	2880/2880=100%	2797/2880=97.1%
Galileo	2880/2880=100%	2742/2880=95.2%
GPS+BDS-3+Galileo	2880/2880=100%	2872/2880=99.7%

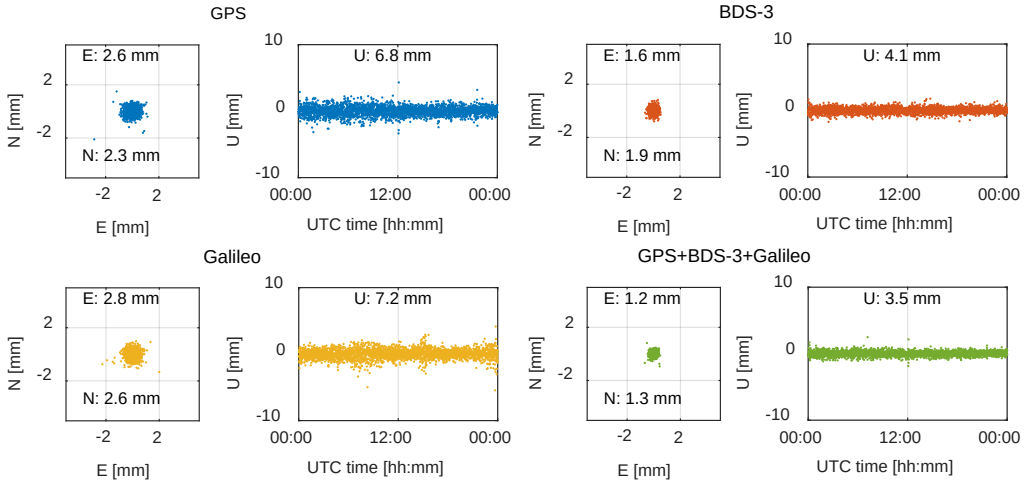

Fig. 4 Horizontal (E = East and N = North) position scatter and vertical (U = Up) time series for the zero baseline APM3-APM7

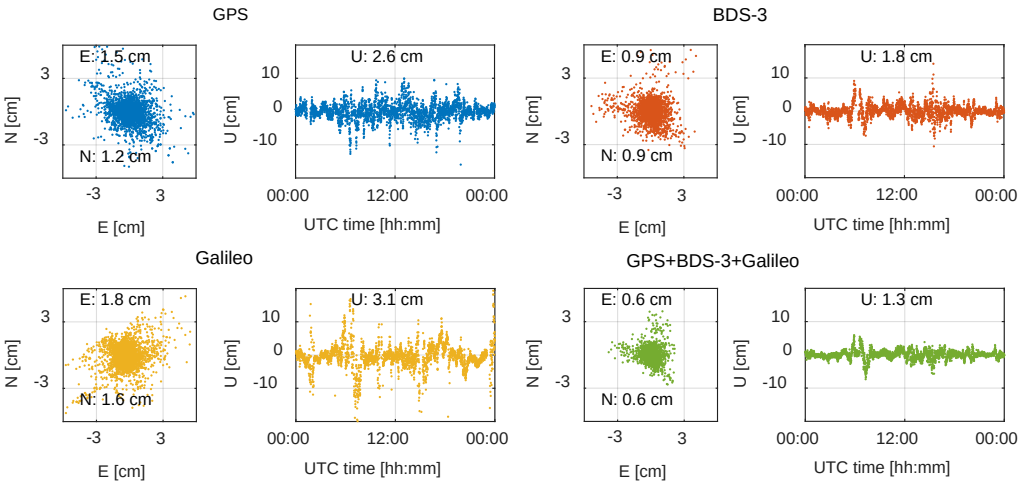

Fig. 5 Horizontal (E = East and N = North) position scatter and vertical (U = Up) time series for the short baseline APM7-WUH2

Based on a zero baseline, we analyzed receiver-related biases in the SD model with GPS, BeiDou navigation satellite system with global coverage (BDS-3) and Galileo, including differential code bias (DCB), differential phase bias (DPB) of the first frequency, and DPB. The number analysis showed two findings. First, the DPB of the first frequency was similar to DCB with centimeter accuracy and can be pre-corrected or estimated as time-invariants in RTK positioning. Second, DPB that is associated with phase observations only thus had sub-millimeter accuracy. However, DPB contained ambiguity of two frequencies, therefore can only be estimated as time-invariants.

With the stability of receiver-related biases, the SD RTK performance of zero and short baselines was tested using GPS, BDS-3 and Galileo in terms of integer ambiguity resolution success rate and positioning accuracy. We found that the SD RTK with BDS-3-only can perform better than GPS-only and Galileo-only as more visible satellites are available. In addition, the SD RTK with GPS+BDS-3+Galileo can achieve higher performance than with a single constellation.

This study preliminarily shows the stability of the receiver-related biases using zero baselines, which can be dynamically constrained to benefit RTK positioning. However, this work is limited to short baselines, and RTK positioning performance for medium and long baselines has not yet been covered. In addition, in multi-constellation scenarios, inter-system bias (ISB) is also a parameter of interest and can be dynamically constrained to improve positioning performance. The understanding and analysis of these works will be a point of interest for future research.

Acknowledgments

Two anonymous reviewers made valuable and helpful comments. Their contributions are highly appreciated.

Data availability

The datasets generated during the current study are available from the author on a reasonable request.

Reference

Atiz O, Shakor A, Ogutcu S, Alcay S (2021) Performance investigation of Trimble RTX correction service with multi-GNSS constellation. Survey Review, 1-11. doi: 10.1080/00396265.2021.1999128

Bahadur B, Nohutcu M (2019) Comparative analysis of MGEX products for post-processing multi-GNSS PPP. Measurement 145:361-369. doi:10.1016/j.measurement.2019.05.094

Hadas T, Hobiger T, Hordyniec P (2020) Considering different recent advancements in GNSS on real-time zenith troposphere estimates. GPS Solutions 24. doi:10.1007/s10291-020-01030-w

Karutin S (2020) The Status of Glonass System. In Proceedings of the 34th International Technical Meeting of the Satellite Division of The Institute of Navigation (ION GNSS+ 2021). doi:10.33012/2020.17553

Khodabandeh A, Teunissen P (2016) PPP-RTK and inter-system biases: the ISB look-up table as a means to support multi-system PPP-RTK. Journal of Geodesy 90:837-851. doi:10.1007/s00190-016-0914-9

Leandro R, Langley R, Santos M (2008) UNB3m_pack: a neutral atmosphere delay package for radiometric space techniquess GPS Solutions 12:65-70. doi:10.1007/s10291-007-0077-5

Leick A, Rapoport L, Tatarnikov D (2015) GPS satellite surveying. Wiley, Hoboken.

Li C, Ching K, Chen K (2019) The ongoing modernization of the Taiwan semi-dynamic datum based on the surface horizontal deformation model using GNSS data from 2000 to 2016. Journal of Geodesy 93:1543-1558. doi:10.1007/s00190-019-01267-5

Liu W, Hu Y, Hsieh T, Zhao J, Wang S (2021) Quinary Offset Carrier Modulations for Global Navigation Satellite System. IEICE Transactions on Communications. doi:10.1587/transcom.2020EBP3121

Liu X, de Jong K, Tiberius C (2003) Reparameterization of single difference and undifferenced kinematic GPS positioning

models. Geo-Spatial Information Science, 6(2), 1-7. doi: 10.1007/BF02826746

Liu X, Tiberius C, de Jong K (2004) Modelling of differential single difference receiver clock bias for precise positioning. GPS Solutions, 7(4), 209-221. doi: 10.1007/s10291-003-0079-x

Mi X, Sheng C, El-Mowafy A, Zhang B (2021) Characteristics of receiver-related biases between BDS-3 and BDS-2 for five frequencies including inter-system biases, differential code biases, and differential phase biases. GPS Solutions 25:1-11. doi:10.1007/s10291-021-01151-w

Mi X, Zhang B, Odolinski R, Yuan Y (2020) On the temperature sensitivity of multi-GNSS intra- and inter-system biases and the impact on RTK positioning. GPS Solutions 24:1-14. doi:10.1007/s10291-020-01027-5

Mi X, Zhang B, Yuan Y (2019a) Multi-GNSS inter-system biases: estimability analysis and impact on RTK positioning. GPS Solutions 23:1-13. doi:10.1007/s10291-019-0873-8

Mi X, Zhang B, Yuan Y (2019b) Stochastic modeling of between-receiver single-differenced ionospheric delays and its application to medium baseline RTK positioning. Measurement Science and Technology 30:095008. doi:10.1088/1361-6501/ab11b5

Odijk D, Nadarajah N, Zaminpardaz S, Teunissen PJG (2017) GPS, Galileo, QZSS and IRNSS differential ISBs: estimation and application. GPS Solutions 21:439-450. doi:10.1007/s10291-016-0536-y

Odijk D, Teunissen P (2008) ADOP in closed form for a hierarchy of multi-frequency single-baseline GNSS models. Journal of Geodesy 82:473-492. doi:10.1007/s00190-007-0197-2

Odijk D, Zhang B, Khodabandeh A, Odolinski R, Teunissen P (2016) On the estimability of parameters in undifferenced, uncombined GNSS network and PPP-RTK user models by means of *S*-system theory. Journal of Geodesy, 90(1), 15-44. doi: 1007/s00190-015-0854-9

Odolinski R, Teunissen P, Odijk D (2015a) Combined BDS, Galileo, QZSS and GPS single-frequency RTK. GPS Solutions 19:151-163. doi:10.1007/s10291-014-0376-6

Odolinski R, Teunissen P (2016) Single-frequency, dual-GNSS versus dual-frequency, single-GNSS: a low-cost and high-grade receivers GPS-BDS RTK analysis. Journal of Geodesy 90:1255-1278. doi:10.1007/s00190-016-0921-x

Odolinski R, Teunissen P (2017a) Low-cost, 4-system, precise GNSS positioning: a GPS, Galileo, BDS and QZSS ionosphere-weighted RTK analysis. Measurement Science and Technology 28. doi:10.1088/1361-6501/aa92eb

Odolinski R, Teunissen P (2017b) Low-cost, high-precision, single-frequency GPS-BDS RTK positioning. GPS Solutions 21:1315-1330. doi:10.1007/s10291-017-0613-x

Odolinski R, Teunissen P, Odijk D (2015b) Combined GPS + BDS for short to long baseline RTK positioning. Measurement Science and Technology 26. doi:10.1088/0957-0233/26/4/045801

Odolinski R, Teunissen P, Zhang B (2020) Multi-GNSS processing, positioning and applications. Journal of Spatial Science 65:3-5. doi:10.1080/14498596.2020.1687170

Paziewski J, Sieradzki R, Baryla R (2018) Multi-GNSS high-rate RTK, PPP and novel direct phase observation processing method: application to precise dynamic displacement detection. Measurement Science and Technology 29. doi:10.1088/1361-6501/aa9ec2

Pignalberi A, Habarulema J, Pezzopane M, Rizzi R (2019) On the development of a method for updating an empirical climatological ionospheric model by means of assimilated vTEC measurements from a GNSS receiver network. Space Weather 17:1131-1164. doi:10.1029/2019sw002185

Ruhl C, Melgar D, Grapenthin R, Allen R (2017) The value of real-time GNSS to earthquake early warning. Geophysical Research Letters 44:8311-8319. doi:10.1002/2017gl074502

Santra A, Mahato S, Mandal S, Dan S, Verma P, Banerjee P, Bose A (2019) Augmentation of GNSS utility by IRNSS/NavIC constellation over the Indian region. Advance in Space Research 63:2995-3008. doi:10.1016/j.asr.2018.04.020

Shen Y, Li B, Xu G (2009) Simplified equivalent multiple baseline solutions with elevation-dependent weights. GPS Solutions 13:165-171. doi:10.1007/s10291-008-0109-9

Shi J, Ouyang C, Huang Y, Peng W (2020) Assessment of BDS-3 global positioning service: ephemeris, SPP, PPP, RTK, and new signal. GPS Solutions 24. doi:10.1007/s10291-020-00995-y

Teunissen P (2018) Distributional theory for the DIA method. Journal of Geodesy 92:59-80. doi:10.1007/s00190-017-1045-7

Teunissen P, Verhagen S (2009) The GNSS ambiguity ratio-test revisited: a better way of using it. Survey Review 41:138-151. doi:10.1179/003962609x390058

Teunissen P (1998) The ionosphere-weighted GPS baseline precision in canonical form. Journal of Geodesy 72:107-117. doi: 10.1007/s001900050152

Teunissen P, deJonge P, Tiberius C (1997) The least-squares ambiguity decorrelation adjustment: its performance on short GPS baselines and short observation spans. Journal of Geodesy 71:589-602 doi: 10.1007/s001900050127

Tian Y, Yuan L, Tan L, Yan H, Xu S (2019) Regularization and particle filtering estimation of phase inter-system biases (ISB) and the lookup table for Galileo E1-GPS L1 phase ISB calibration. GPS Solutions 23. doi:10.1007/s10291-019-0908-1

Tuka A, El-Mowafy A (2013) Performance Evaluation of Different Troposphere Delay Models and Mapping Functions. Measurement 46:2, 928–937. doi:10.1016/j.measurement.2012.10.015

Xiao G, Li P, Sui L, Heck B, Schuh H (2019) Estimating and assessing Galileo satellite fractional cycle bias for PPP ambiguity resolution. GPS Solutions 23. doi:10.1007/s10291-018-0793-z

Yalvac S, Berber M (2018) Galileo satellite data contribution to GNSS solutions for short and long baselines. Measurement 124:173-178. doi:10.1016/j.measurement.2018.04.020

Yang Y, Liu L, Li J, Yang Y, Zhang T, Mao Y, Sun B, Ren X (2021) Featured services and performance of BDS-3. Science Bulletin 66:2135-2143. doi:10.1016/j.scib.2021.06.013

Yuan Y, Mi X, Zhang B (2020) Initial assessment of single-and dual-frequency BDS-3 RTK positioning. Satellite Navigation. 1(1):1-7. doi: 10.1186/s43020-020-00031-x

Zaminpardaz S, Wang K, Teunissen P (2018) Australia-first high-precision positioning results with new Japanese QZSS regional satellite system. GPS Solutions 22. doi:10.1007/s10291-018-0763-5

Zha J, Zhang B, Liu T, Hou P (2021) Ionosphere-weighted undifferenced and uncombined PPP-RTK: theoretical models and experimental results. GPS Solutions 25. doi:10.1007/s10291-021-01169-0

Zhang B, Chen Y, Yuan Y (2019) PPP-RTK based on undifferenced and uncombined observations: theoretical and practical aspects. Journal of Geodesy 93:1011-1024. doi:10.1007/s00190-018-1220-5

Author Biographies

Xiaolong Mi is a Ph.D. candidate at the Innovation Academy for Precision Measurement Science and Technology, Chinese Academy of Sciences, China and Curtin University, Australia. His research focuses on high-precision GNSS positioning, time and frequency transfer with integer ambiguity resolution, multi-GNSS inter-operability and software development.

Baocheng Zhang is a professor at the Innovation Academy for Precision Measurement Science and Technology, Chinese Academy of Sciences. His research focuses on modeling multiple global navigation satellite systems for integer ambiguity resolution-enabled precise point positioning (PPP-RTK) applications.

Yunbin Yuan is a professor and the director of the GNSS Application and Research Group at the Innovation Academy for Precision Measurement Science and Technology at the Chinese Academy of Sciences. His current research interests are the following: (1) GNSS-based spatial environmental monitoring and analysis, (2) high-precision GNSS satellite navigation and positioning, and (3) GNSS applications to orbit determination for LEO satellites.